Supporting Information

Phosphazene-Derived Stable and Robust Artificial SEI for Protecting Lithium Anodes in Li-O_2 Batteries

Wen-Long Bai,[a] Zhen Zhang,[a] Xin Chen,[a] Qiang Zhang,[a] Zhi-Xin Xu,[a] Guang-Yao Zhai,[a] Xiu Lin,[a] Xin Liu,[a] Tsegaye-Tadesse Tsega,[a] Chuan Zhao,[b] Kai-Xue Wang,[a] Jie-Sheng Chen[a]*

[a] Shanghai Key Laboratory for Molecular Engineering of Chiral Drugs, School of Chemistry and Chemical Engineering, Frontiers Science Center for Transformative Molecules, Shanghai Jiao Tong University, Shanghai 200240, P. R. China
Email: k.wang@sjtu.edu.cn

[b] School of Chemistry, The University of New South Wales, Sydney, NSW 2052, Australia

Experimental section

Materials

NaH, 2,2,3,3,4,4,5,5-Octafluoro-1-Pentanol and trifluoroethanol, and tetrahydrofuran (THF) were purchased from Adamas. Phosphazene and Ketjen black (KB, EC600JD) were purchased from Titan. CR2025 coin cells were purchased from X2 LAB Pte Ltd.

Synthesis of Sodium 2, 2, 3, 3, 4, 4, 5, 5-Octafluoro-1-Pentanol (SOP) and Sodium trifluoroethanol (ST).

0.04 mol NaH was dissolved in a solution including 50 mL tetrahydrofuran (THF) under stirring in a N_2 atmosphere. Then, 50 mL THF containing 0.04 mol 2,2,3,3,4,4,5,5-Octafluoro-1-Pentanol was dropped wise into the above solution. SOP was prepared after the formation of a transparent solution. The ST was prepared through the reaction between trifluoroethanol and NaH following the procedure

described above.

Synthesis of ASEI-Li.

0.05 mol of phosphazene was dissolved in 20 mL THF. 0.15 mol SOP was dropped into the above solution and the mixed solution kept stirring for 12 h. Then, ST was dropped in the mixed solution under a temperature within 50 ℃ for 12 h. The mixed solution was dropped on the surface of Li metal at 60 ℃. The ASEI-Li was obtained after 0.5 h or 1.0 h. Then the ASEI-Li metals were washed with DME and dried under vacuum for 15 mins. All processes were done in an argon-filled glove box with O_2 and H_2O content below 1.0 ppm.

Preparation of Li–O_2 batteries.

Ketjen black (KB, EC600JD) was served as cathode for Li-O_2 batteries. The loading mass of KB on the carbon cloth was 0.1-0.3 mg cm^{-2}. CR2025 coin cells with 17 holes for the permeation of O_2 were assembled with as-prepared KB cathodes, ASEI-Li (15 mm in diameter), glass fiber separator, and 1.0 M LiTFSI/TEGDME electrolyte in an Ar-filled glove box.

Electrochemical measurement.

The galvanostatic charge-discharge performance was evaluated in a O_2-filled glove box with the potential ranging from 2.0 to 4.3 V by a battery tester (LAND CT2001) at room temperature. The CV tests were carried out within a voltage range of 2.0 and 4.5 V. The cycling ability was evaluated at the current density of 400 mA g^{-1} with cut-off capacity 1000 mAh g^{-1}. Electrochemical impedance spectroscopy (EIS) measurement was conducted on a CHI 660C with a frequency extent of 0.01-10^5 Hz.

The Li (with 10 holes) stripping/plating performances were collected using symmetric cells (anode with 17 holes) assembled at a current density of 0.2, 0.5, 1.0 mA cm^{-2} in O_2 by a battery tester (Neware).

Characterization.

X-ray diffraction (XRD) patterns were recorded on a D/max 2550VL/PC X-ray diffractometer (Rigaku, Japan) equipped with Cu Kα radiation (λ = 1.5418 Å, 40 kV, 30 mA). The discharged/charged electrodes, on-top and cross-sectional topography of Li metal were observed on a field-emission scanning electron microscope (FESEM, NOVA Nano SEM 230, FEI, USA). Fourier transform infrared spectroscopy (FTIR) analyses were performed on an FTIR spectrometer (Nicolet6700) from 2000 to 700 cm^{-1}. ^{1}H-cross-polarization magic-angle spinning (CPMAS) nuclear magnetic resonance measurements were performed on a Bruker Avance Ⅲ 400 MHz system. The electrolytes of Li-O_2 batteries were collected by washing the glass fiber separators with D_2O, and subjected to ^{1}H NMR (Bruker, 500 M). XPS analysis was performed by a Kratos Axis UltraDLD spectrometer (Shimadzu Group Company, UK) with a monochromatic Al Kα source. The inner chemical compositions of the ASEI were characterized by XPS depth profile tests, which were conducted by using Ar sputtering at different time from 0s to 1000s. The estimated sputtering rates were approximately 0.013 nm s^{-1}. The AFM tests were conducted by dimension icon & FastScan Bio. The peak force quantitative nanomechanics (PF-QNM) mode, an extension of PFT mode, was used to measure the Young's modulus of the Li. In the PF-QNM mode, the Young's modulus, E*, is obtained by fitting the retracting curve

using the Derjaguin-Muller-Toporov (DMT) model given by:

$F_{tip}=0.75E^{*}(Rd^{3})^{1/2}+F_{adh}$

where the F_{tip} is the force on the tip, R is the tip end radius, F_{adh} is the adhesion force, and d is the tip sample separation. The value of E* can be directly decided by these parameters. The analysis of the DMT model was performed by the Nanoscope Analysis software.

Computational Methods

In this work, DFT calculations were carried out with the Gaussian09 software package. HSE06 method with def2-TZVP basis set was applied to calculate the HOMO and LUMO values of all molecules involved as reported by previous works.

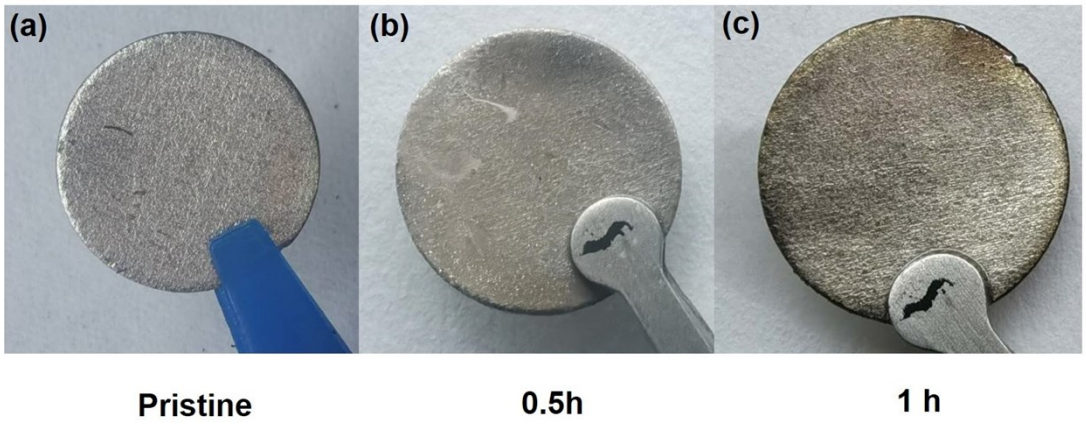

Fig. S1. Photographs of (a) pristine Li metal, (b) ASEI-Li metal (0.5h), and ASEI-Li metal (1.0h).

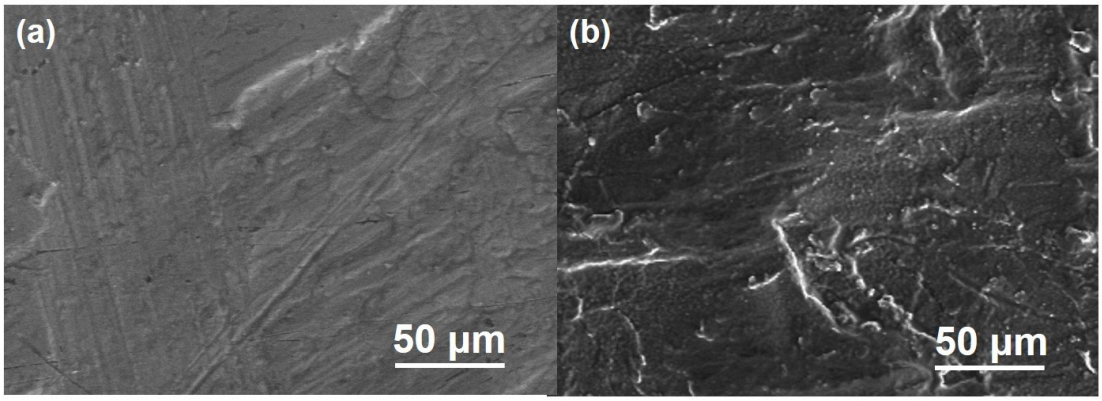

Fig. S2. SEM images of (a) ASEI-Li (0.5 h) and (b) ASEI-Li (1.0 h) metal.

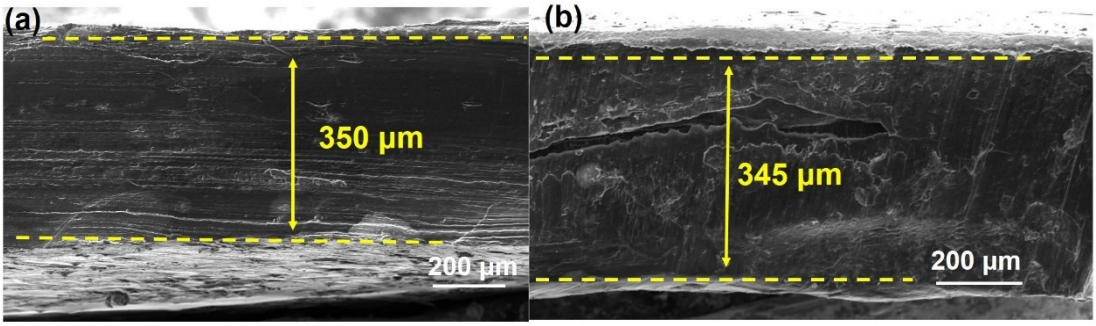

Fig. S3. Cross-sectional SEM images of (a) ASEI-Li (0.5 h) and ASEI-Li (1.0 h).

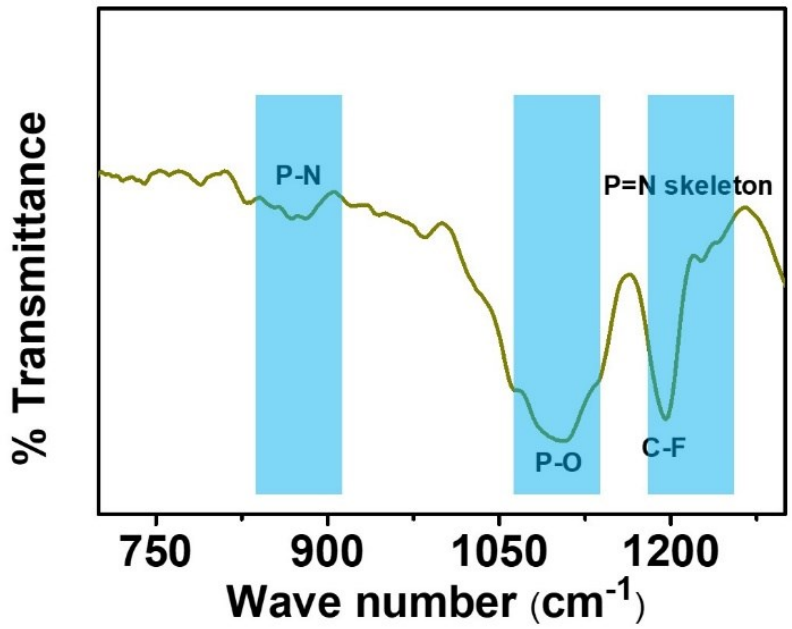

Fig. S4. FTIR spectra of the ASEI-Li.

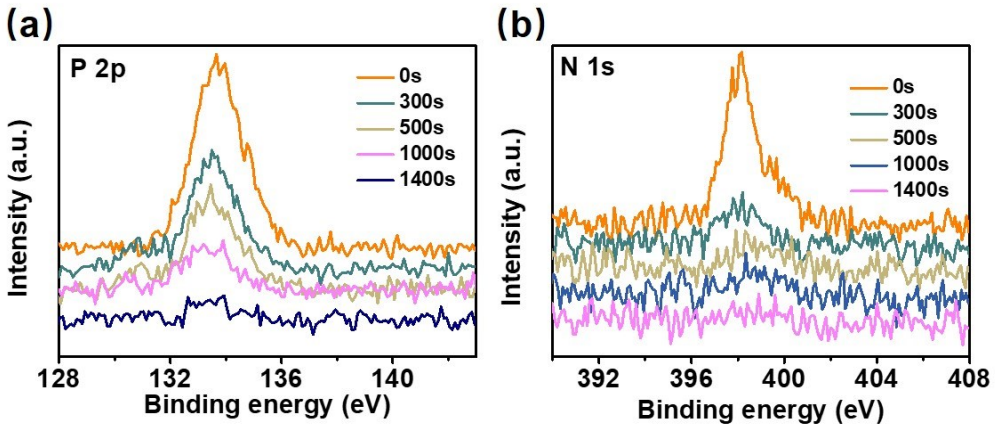

Fig. S5. N 1s and P 2p XPS spectra of the ASEI with different sputter time from 0s to 1400s.

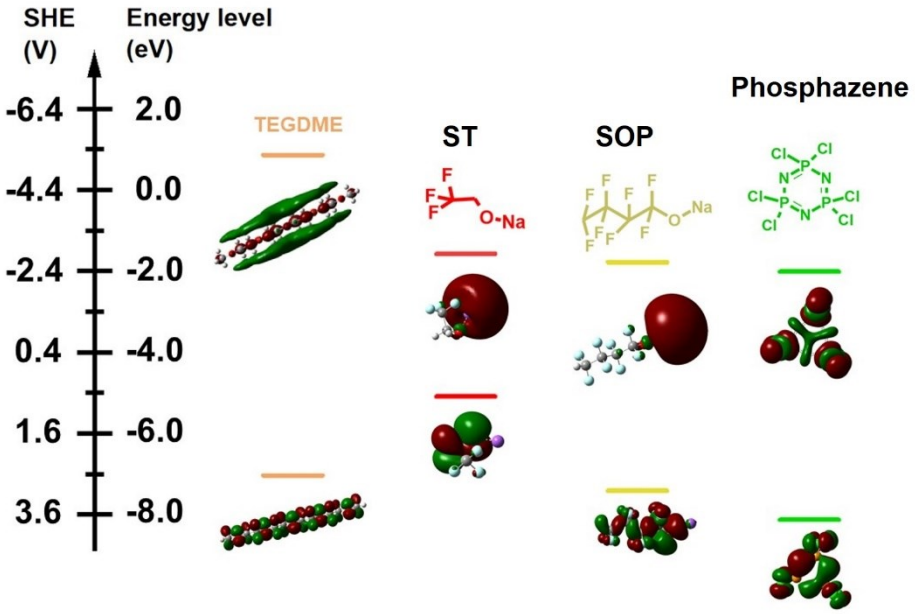

Fig. S6. LUMO and HOMO energies of TEGDME, phosphazene, SOP, and ST by DFT calculations. The green and red regions represent the negative and positive phases of the molecular orbitals, respectively.

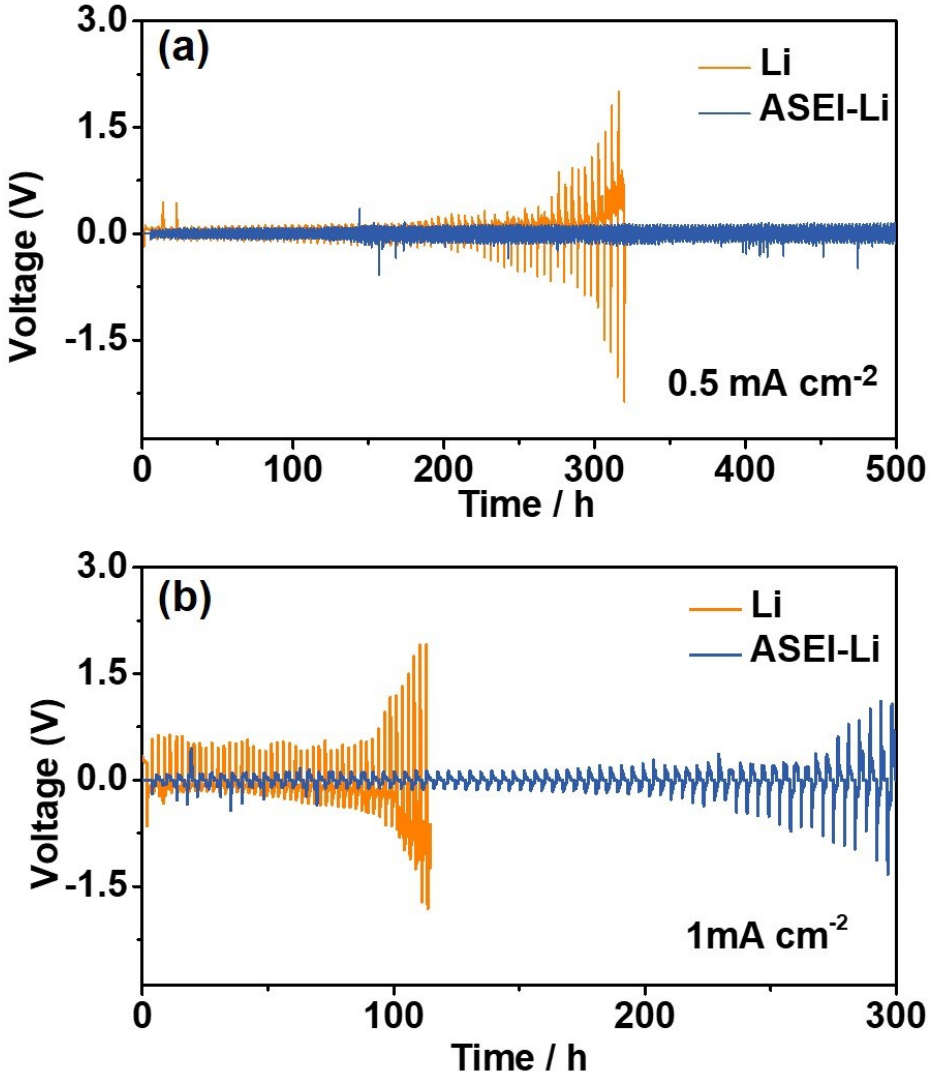

Fig. S7. Voltage-time profiles of the Li plating/stripping of the symmetric cell with bare Li metal, ASEI-Li ((a) 0.5 mA cm^{-2} and (b) 1.0 mA cm^{-2} for 1 h for each plating/stripping process)

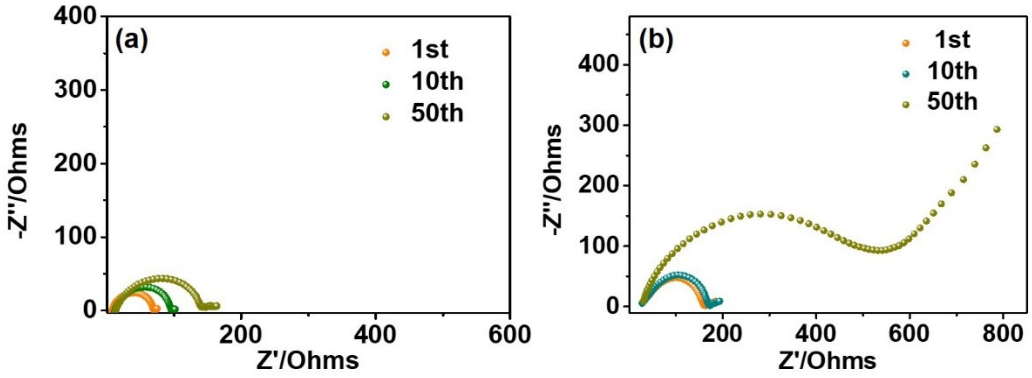

Fig. S8. EIS of symmetric cells coupled with (a) ASEI-Li and (b) Li cycled at a current density of 0.2 mA cm^{-2}.

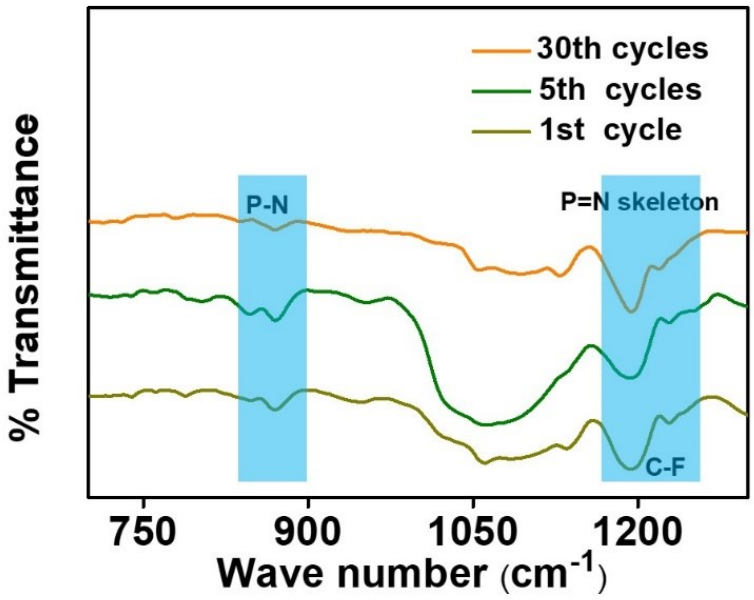

Fig. S9. FTIR spectra of the ASEI-Li in the symmetric cells m at 0.2 mA cm^{-2} after different cycles.

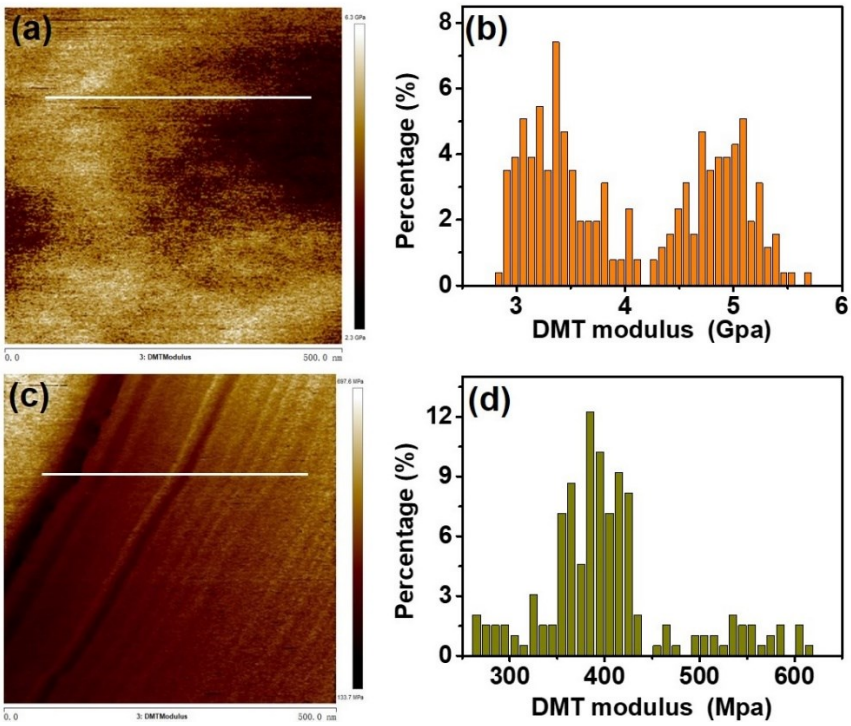

Fig. S10. (a,c) 2D distribution and the (b,d) quantitative statistics of the Young's modulus of the SEI of (a,b) ASEI-Li and (c,d) Li cycled at 0.2 mA cm^{-2} in the symmetric cells for 10^{th} cycles.

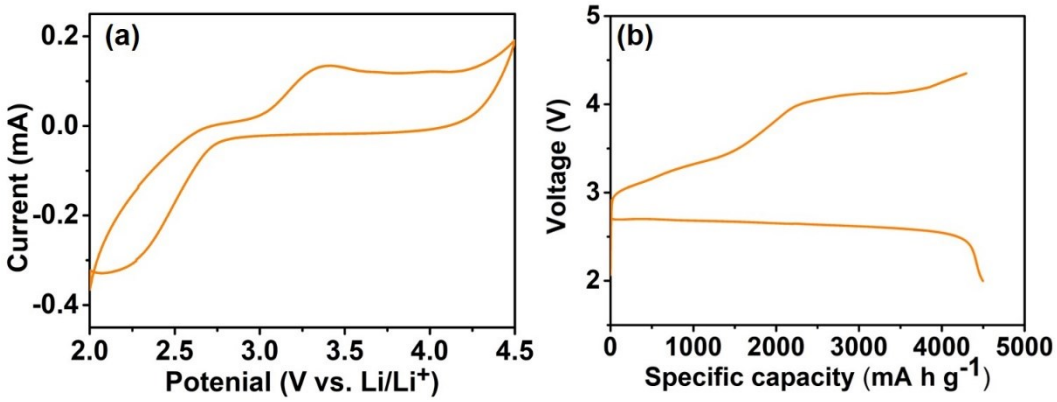

Fig. S11. (a) CV curves of Li−O_2 batteries with ASEI-Li under O_2 atmosphere in the range of 2.0 V to 4.5 V. (b) Full discharge/charge profiles of Li–O_2 batteries with ASEI-Li at current density of 100 mA g^{-1}.

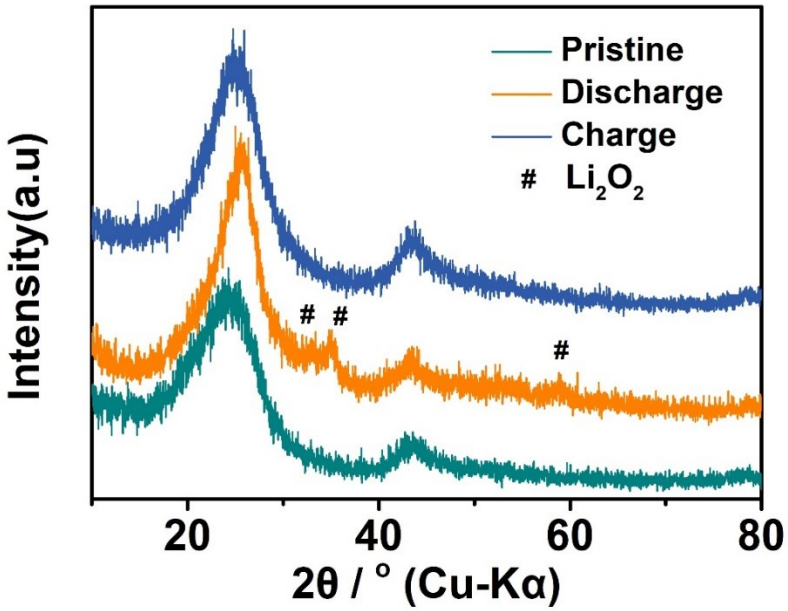

Fig. S12. XRD patterns of the pristine, discharged and charged KB cathodes.

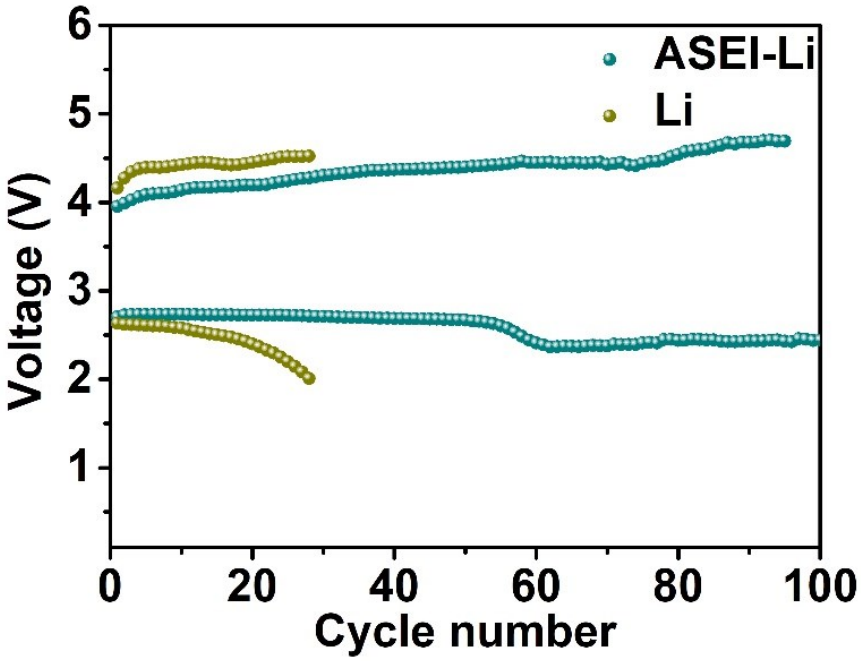

Fig. S13. Charge and discharge terminal potential of Li–O_2 batteries with Li and ASEI-Li at a current density of 400 mA g^{-1} with a limited capacity of 1000 mAh g^{-1}.

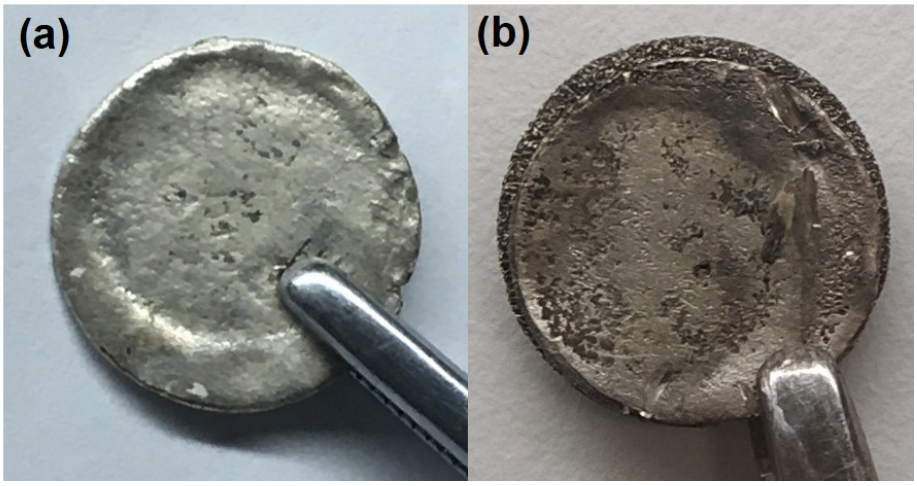

Fig. S14. Photographs of (a) the ASEI-Li anode after discharged/charged for 100 cycles and (b) Li anode after discharged/charged for 28 cycles of Li-O_2 batteries.